中国科学院上海应用物理研究所

数据分析备忘录兼毕业设计素材

数据分析日志

Author:
金小海

Supervisor:
自己

上海市嘉定区嘉罗公路 *2019* 号
上海应用物理研究所

核物理研究室

2018 年 5 月 23 日

序

目录

第1章 STAR scheduler-User Manual

1.1 Introduction

The STAR scheduler was developed to allow users to submit a job on several input files. residing on NFS of on the various local disks of the farm machines. The scheduler will divide the job into different processes that will be dispatched to different machines. In order for the scheduler to do that, the user has to follow some simple rules when writing his program, and to write an XML file describing the job he wants to be done.

In this manual we show the steps the user needs to take to use the scheduler.

1.2 An example

1.2.1 Preparing the program

What will you basically submit to the scheduler is a command line. The program will have to receive instruction from the scheduler which input files it should use. For your convenience, there are two ways this is done.

1.2.1.1 Getting the input files from the filelist

The scheduler will generate a file list like this for each process:

```
/star/data21/reco/productionCentral/FullField/P02gc/2001/312/st_physics_2312011_ra
/star/data21/reco/productionCentral/FullField/P02gc/2001/312/st_physics_2312011_ra
/star/data21/reco/productionCentral/FullField/P02gc/2001/312/st_physics_2312011_ra
```

The environment variable $FILELIST will be set to the name of the file list. You can use this variable on the command line to retrieve the name as a parameter of your program. For example, submitting cat $FILELIST will display in the standard out all the input files that were assigned to that particular process.

Be careful that the output file is different for every process it might be dispatched, otherwise two processes that were dispatched to different machines and are running in the same moment will interfere with each other. You can, for example, have the name of the output files depend on the filelist name, or from the job ID, which you can retrieve from the environment variable $JOBID. In case you have an output file for each input file, and all your input files have different names, you can have the output file depend on the particular input. All the input files are assigned to only one process.

1.2.1.2 Getting the input files from environment variables

Another way to retrieve the file list is to look for the $INPUTFILECOUNT variable that tells you how many files where assigned to the process. Then you can look for the $INPUTFILE0...$INPUTFILEn for each input file name. Also here you have to be careful for the output file names.

1.2.2 Job description

Once your program is ready, you can write the job description. A job description looks like this: The first line tells the parser what set of characters

```
PASS
```

图 1.1: jobDescription

was used. Don't worry about it. If you are not used to XML, you can see that there are some tags that open and close. The main tag you see is <job> that closes at </job>. It means that everything inside that describes a job. You could have more than one, but you won't need to do that. Not having specified the working directory, the current directory will be used.

Inside the job, you can see another tag <command>. Inside that you will put the command line you will want to be executed. Then you have the <stdout> tag: it tells where the output of the process will be saved. After that you see many <input> tags. These don't have a </stdout> or </input> because they are directly closed at the end (notice the '/'in the ending '/>'). URL is an attribute of all the tags that will specify a file (input, stdout, stdin, stderr). For example, in the first input tag you are telling the scheduler that you require that file as an input for your job. After "file:"you have to put a full path to an NFS mounted file.

There are other options you can specify in your job description, and you can find the details later in this manual.

1.2.3 job submit

Once you have prepared your XML file, you are ready. You just type:

```
star-submit jobDescription.xml
```

where jobDescription.xml is the name of the file that contains your job description. In this version, you have to specify the position of the star-submit command. In the final version, that won't be required.

The scheduler will create the scripts and the file lists for the processes. These will be created in your directory. Also this will change in the final version, and they will be put in a scratch directory.

1.3 Job description specification

Here is the full specification of what the XML for the job description can contain.

1.3.1 XML syntax

You don't need to know XML very well to understand how to use the scheduler. For the sake of being complete, here are a few concept that you will see in this description. It's not necessary to know them, but since XML

is being more and more used, it might satisfy a general curiosity. Remember that HTML is kind of a subset of XML.

The basic notion in XML is the element (or entity), which is basically two tags with the same name: a start tag and an end tag. For example, <job>…</job> is an element.

An element can have some attributes, that better specify it. For example, in <job title="My title"> title is an attribute of the job element. The attributes are specified in the start tag.

An element generally contain some data, that can be other elements, or just some text, for example in:

```
<job> <command>echo test</command> </job>
```

The element job contains the element command that in turn contain the data "echo test". An element can also contain no data at all, and just have some attributes. For example, in <input URL="file:/star/u/carcassi/myfile"/> we have the element input, with a URL attribute, the ends right away. That is the start tag and the end tag are put together in one tag (notice the '/' in the end).

That is all the XML we are using in the scheduler.

1.3.2 the <Job> element

Here is an example of the <job> element with all the attributes:

```
<job simulateSubmission ="true" mail="true">
...
</job>
```

The <job> element can be have the following attributes 1.1:

Below is a list of dispatcher and the job tag attributes each supports. It should be noted that the attributes (simulateSubmission, nProcesses, maxFilesPerProcess, minFilesPerProcess, filesPerHour, fileListSyntax, inputOrder) are supported by all dispatchers, as they are observed at a higher level 见链接.

1.3.3 The <command> element

The <command> element doesn't have any attributes, and the data that it contains is the actual command script that will be submitted using a csh script.

表 1.1: The attributes of <job> element

Attribute	Allowed values	Meaning	Default
datasetPlitting	“eventBased” or “fileBased”	见链接	“fileBased”
splitBy	Any Catalog key	见链接	none
simulateSubmission	“true” or “false”	见链接	false-by default the jobs are submitted
name	any string	见链接	none
mail	“true” or “false”	见链接	false-by default no mail is allowed
nProcesses	any integer	见链接	Determined by the input
maxEvents	any integer	见链接	infinite
minEvents	any integer	见链接	N/A
softLimits	“false”	见链接	false
maxFilesPerProcess	any integer	见链接	Infinite
minFilesPerProcess	any integer	见链接	N/A
eventsPerHour	integer of floating point	见链接	Infinite
filesPerHour	intgeger or floating point	见链接	Infinite
filesListSyntax	“paths” or “rootd” or “xrootd”	见链接	paths
inputOrder	a string that is a catalog attribute	见链接	none

第2章　奇异粒子 (K^0_S, Λ+$\bar{\Lambda}$, Ξ^-+Ξ^+) 的重构

2.1　介绍

In these collisions, atomic nuclei (heavy-ions) moving at nearly the speed of light collide and deposit a large amount energy in a small region of space where the temperature and density is comparable with that existed in the early universe approximately on microsecond after the Big Bang. These are six different types, or flavors, of quarks: u(up), d(down), s(strange), c(charm), t(top), b(bottom). Nucleons only carry the lightest quarks u and d. The hadrons carrying strange quarks are strange hadrons. Quarks have another important degree of freedom, known as color, just as electic charge to electrons. A color is assigned to each quark, for example, R(red), G(green) and B(blue). All hadrons are colorless objects. The forces between colored quarks are called strong interactions which is well described by Quantum ChromoDynamics(QCD).

2.2　Nucleus-Nucleus Collisions Dynamics

A high energy head-on nucleus-nucleus collision can be viewed in the laboratory frame as two thin disks approaching each other at nearly the speed of light because of the Lorentz contraction effect in the moving direction. While a precise theoretical descrition of the collision dynamics is diffcult to find, it is generally believed the ultra-relativistic heavy-ion collision has four stages of the evolution as shown in Fig. 1.4: pre-equilibrium parton cascade, an equilibrated QGP, hadronization and freeze-out of hadrons. After the collision of two nuclei(Au + Au at RHIC) at $(z,t) = (0,0)$, the energy density may be sufficiently high for the fromation of deconfined quarks and gluons, a cascade of colliding partons. This partonic state initically may not be in thermal equi-

librium, but the interaction between partons eventually bring the system into a local equilibrium at the proper time τ_0 when the QGP is formed. Then the QGP expands and its temperature drops down with increasing time. The hadronization process takes places at a time in the order of $10\tau_0$. This stage involves the formation of hadrons and hadrons continue to interact with each other. As the system expanding further, the interactions between the hadrons stop and the hadrons stream out of the collision region and the temperature falls below the freeze-out point.

Experimentally, since the direct probe of the QGP and hadronization process is not possible, the measurement of the particles in the final stage is the only way for us to study the formation and evolution of the QGP at the early stages. The initial energy density ε right after the collision can be determined according to the produced particles.

PASS

图 2.1: 核核碰撞的时空演化图.

$$\varepsilon = \frac{m_T}{\tau_0 A}\frac{dN}{dy}|_{y=0}. \tag{2.1}$$

where $m_T = \sqrt{m^2 + p_T^2}$ is the transverse mass of the particles produced, m and p_T are the mass and the transverse momentum of the particles, respectively. A is the overlapping area of two colliding nuclei and $\frac{dN}{dy}|_{y=0}$ is the number of hadrons pe unit rapidity. The τ_0, the proper time of thermalizing initial partons, may depend on the colliding beam energy and is believed to be on the order of 1 fm/c. For Au+Au collisions at RHIC, most produced particles are pions. The energy density ε is about 4.6 GeV/fm^3 for Au+Au collision at $\sqrt{s_{NN}} = 130GeV$ and $5.0GeV/fm^3$ for $\sqrt{s_{NN}} = 200GeV$ at RHIC. These estimates of the energy density exceed the critical density for the QGP formation, $1.0GeV/fm^3$, calculated from lattice QCD.

2.3 Collision Geometry

Different from proton-proton collisions, nuclear collisions can be reliably classified according to their centrality - a variable measuring the degree of over-

lapping between two colliding nuclei. Centrality is closely related to the impact parameter b that is defined as the transverse distance between the centers of the two colliding nuclei in a nucleus-nucleus collision as illustated in **??**. Al-

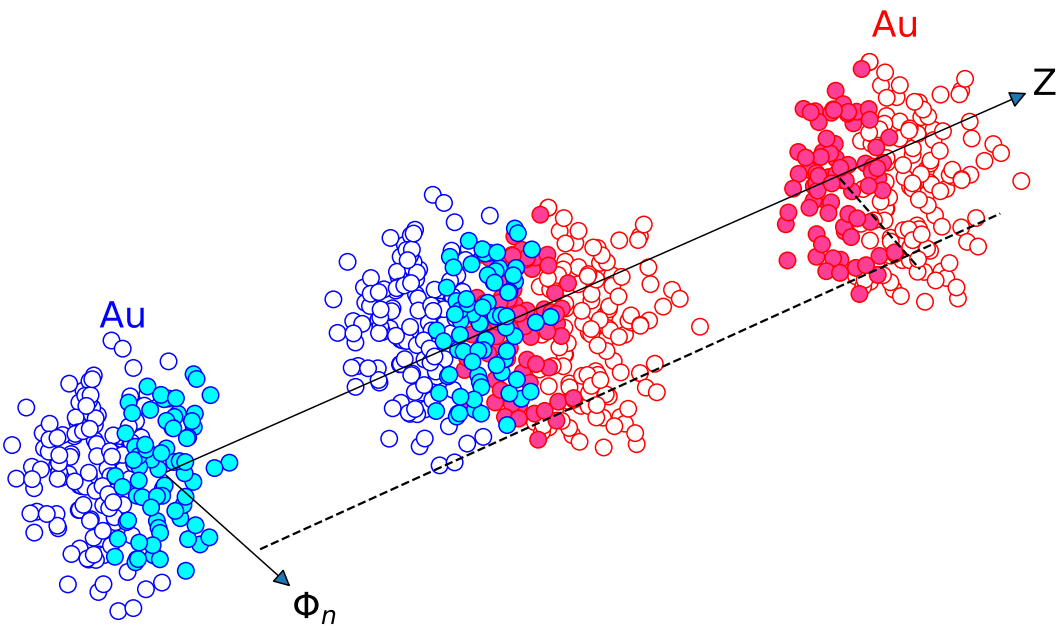

图 2.2: Nuclear collision geometry and centrality for Au+Au collision.

thouth b cannot be directly measured in experiments, it has been widely used in theoretical models. N_{part} is another critical parameter in nuclear reactions and is a function of b. Roughly speaking, a head-head collision with a small b involves more colliding nucleons, thus a large N_{part}. For the most central collisions, the impact parameter $b = 0$ and $N_{part} \approx A + A$. The probability of this kind of collisions is very small, therefore corresponding to a top percentage (a few %) of centrality. Another similar collision parameter, N_{binary}, represents the number of equivalent nucleon-nucleon collisions in a nucleus-nucleus collision. N_{part} and N_{binary} can be obtained from model calculations. At STAR, the centrality is determined by measuring the charged particle multiplicity, N_{ch}, for Au+Au and d+Au collisions. Larger N_{ch} corresponds to more central collisions. For example, in Au+Au 200GeV collisions the centrality $0-5\%$ at STAR means the top 5% events that have the averaged $N_{ch} > 686$ in middle rapidity region($|y| < 0.5$).

2.4 Transverse Mass(Momentum) Spectra

In heavy-ion collisions people are more interested in the invariant transverse mass(momentum) spectrum at a specific rapidity region,

$$\frac{d^2N}{2\pi p_T dp_T dy} \tag{2.2}$$

At low p_T(< 2 GeV/c) in nucleus-nucleus or $p(d)$-nucleus collisions, the spectrum can be well fitted by an exponential function in m_T

$$\frac{d^2N}{2\pi m_T dm_T dy} \propto e^{-\frac{m_T-m}{T}}. \tag{2.3}$$

according to thermal models in which a large body of thermal hadronic or patonic matter is thought to act as a source of produced particles. The fit parameter T, usually called temperature, is directly related to the freezeout temperature. A large T means a earlier freezeout for a specific particle. The heavy multi-strange hadrons, like the Ω and charmed hadrons, are good particles for probing the QGP since they have large T and thus carry early early evolution information, probably at the stage of the chemical freeze-out. The hydrodynamic models have been successfully used to described the collective flow behavior at the low p_T region. The evolution of the flow is treated as an ideal fluid. The flow velocity can be obtained by fitting the spectrum with Blast wave function.

然而, 对于高 p_T(> 2 GeV/c) 区间, 热模型核流体模型都无法较好的进行解释. 微扰 QCD(pQCD) 运用 parton scattering, gluon shadowing and jet quenching 等方法可以进行有效的描述. 这些方法导致一个较硬的 p_T 谱 (更加的平缓), 其谱的分布可以被指数函数进行拟合

$$C(1+\frac{p_T}{p_0})^{-n} \tag{2.4}$$

In the heavy-ion collisions, any approach trying to reproduce the experimental data successfully has to deal with the dominant dynamical mechanism for the colorred low p_T(soft) and high p_T(hard) region separately.

2.5 核的修正因子 R_{CP} 和 R_{AA}

It is believed that the QGP would be more likely to be created in central nucleus-nucleus collisions. In peripheral collisions, where hte number of effect colliding nucleons is small, the created matter is not sufficiently large to reach thermalization. Nuclear effects can be investigated by measuring a nuclear modification factor, the particle yield ratio from the central to peripheral collisions:

$$R_{CP}(p_T) = \frac{[(dN/dp_T)/N_{binary}]^{Central}}{[(dN/dp_T)/N_{binary}]^{Peripheral}} \tag{2.5}$$

其中,N_{Binary} 是初始的核反应过程中, 核核 (nucleon-nucleon) 碰撞的次数 for each nuclear collision. 类似于 R_{CP}, 另一个类似的核修正参数定义为核子碰撞

PASS

图 2.3: R_{CP} 的 p_T 依赖.

的产额与质子碰撞的产额比.

$$R_{AA}(p_T) = \frac{d^2N/dp_Td\eta}{T_{AA}d^2\sigma^{pp}/dp_Td\eta} \tag{2.6}$$

其中 η 是赝快度,$T_{AA} =< N_{binary} > \sigma^{NN}_{inel}$. R_{AA} 取 pp 碰撞作为参考.

2.6 Ehancement of Strange Hadrons

A massive strangeness quark, s 被认为对与 QGP 的信号是极其敏感的, 因为其质量极其的靠近理论计算的相变临界温度值 T_c, 这就意味着奇异性强子的测量可以很好的提供退禁闭时的信息. 在退禁闭相时, 奇异夸克可以通过 $(g + g- > s\bar{s})$ 来产生, 通过该胶子反应道, 奇异性核子产额的增多被认为是 QGP 存在的验证探针.

2.7 探测器

Four kinds of charged particles, $\pi^+(\pi^-), K^+(K^-), p(\bar{p}), e(\bar{e})$ can be identified via the measurement of ionization energy loss (dE/dx) of the particle travelling across the TPC. Other neutral and charged particles, like the $K^0_s, \Lambda(\bar{\Lambda}), \Xi^-(\Xi^+)$

and $\Omega^-(\Omega^+)$ 可以通过弱衰变进行重构. The vector meson ϕ can be measured up to $p_T = 6GeV/c$ using event-mixing technique. The EMC, designed to measure high energy ($\geq 2GeV$) electrons and photons, is used to identify some particles decaying to electrons and photons, such as π^0, η and J/Ψ.

2.8 分析方法

In the STAR TPC, four particles(electictrons, pions, kaons and protons) in the low p_T region can be identified through their energy loss rate(dE/dx) along their track in the TPC, while other particles are reconstructed from them through decay channels. K^0_S, Λ, Ξ^- and their anti-particles decay to pions and protons through their weak decay channels. These involves a relatively long decaying time leading to a large decay length. Therefore, the daughter particles (pions and protons) were created at some point in space away from the primary vertex. This feature can be used to get rid of much background and makes these strange hadrons easy to reconstruct.

2.8.1 minimum bias data

To remove trigger biases, the minimum bias also require a vertex-z cut within 50 cm of the TPC center. Moreover, primary vertices (collision points) were not successfully reconstructed in some events due to the low multiplicity (number of particles from one event) in the TPC so that these events are useless.

2.8.2 Centrality definition

Nuclear effects are different for the different collision centralities, which are related to the impact parameter b of the collision in geometry. In experiments we define the centrality according to the number of charged particles measured in a given rapidity region. These tracks must be from minimum bias events with primary vertex found. The qualified tracks for the centrality definition are the charged primary tracks with the following requirements:

- fit points >= number.(拟合点大于某个值).

- 某个快度或者赝快度区间.
- p_T 小于某个区间.
- a distance of closest approach (DCA) to the primary vertex 小于某个距离.

PASS

图 2.4: RefMult

根据 reference multiplicity (N_{ch}) 来定义中心度.

2.8.3 径迹的选择

There are two sets of tracks available for the analysis in the STAR.

Primary tracks Primary tracks requiring a distance of closest approach (DCA) to the primary vertex less than 3 cm are usually used for identification of particles originating at or very close to the primary vertex.

Global tracks Global tracks that include all the TPC tracks are mainly used to reconstruct particles that decay at some point in space away from the primary vertex.

对于 K^0_s, Λ, Ξ^- 以及它们的反粒子, 因为较长的衰变距离, 所以一般使用 Global tracks 来做重构的分析. The number of hit points for each track ranges from 8 to 45. We required at least 16 hit points for a track of good quality and discarded short tracks that might be split from a track with a large number of hit points. To reduce the background for these reconstructed particles, the $n\sigma$ criterion cuts on their daughter tracks is used.

$n\sigma$ criterion A parameter describing how far the measured dE/dx deviates from the theoretical value of a known particle.

2.8.4 V0 重构

V0 粒子的衰变道和衰变分支比见9.1. The fact that V0 particles decay at some point away from the primary vertex allows us to build the signals by applying appropriate topology cuts. 下图为 V0 衰变的 x-y 平面示例图 The

图 2.5: V0decay

trajectory of the charged daughter tracks, is a helix, that is, a circle in the x-y plane plus a constant velocity in the Z direction.

To find V0s, we first need to calculate the distance of closest approach(DCA) between two daughter tracks (DCA $P^+ + P^-$). Theoretically DCS $P^+ + P^-$ should be zero if two daughter particles are decayed from the V0. Practically a distance tolerance is, however, allowed due to the track position resolution. We allow this DCA to be less than 1 cm. The detailed math derivation for calculating DCA $P^+ + P^-$ was published in [1].

Similarly, a tolerance is applied to the DCA between the V0 and the primary vertex (DCA_V0_PV) even for a V0 coming from the primary vertex.

- All the K^0_s particles are assumed to have been produced at the primary vertex, so we set the limit for K^0_s DCA_V0_PV as 1cm.
- However, some of $\Lambda(\bar{\Lambda})$ can be produced at the secondary vertex via the $\Xi(\bar{\Xi})$ weak decay channel, which forces us to use a larger DCA_V0_PV cut.

The other two DCAs, DCA of P^+ to primary vertex (DCA_P+_PV) and DCA of P^- to primary vertex (DCA_P−_PV), can be used to reduce the background efficiently by cutting away a large portion of primary tracks which have small DCA_P+_PV or DCA_P−_PV.

V0 粒子的动量方向由径迹 $P+$ 和径迹 $P-$ 在衰变顶点的动量之和决定. 衰变长度表示为衰变顶点和初级顶点之间的距离. V0 的不变质量 (m) 由 daughter 径迹的质量和动量决定:

$$m = \sqrt{(\sqrt{m_+^2 + P_+^2} + \sqrt{m_-^2} + P_-^2)^2 - P^2}, \tag{2.7}$$

其中 $m_+(m_-)$ 是正负径迹粒子的质量, P_+ 是正径迹的动量, P_- 是负径迹的动量, P 是 V0 粒子在衰变顶点的质量.

2.8.5 不变质量谱和背景估计

The K^0_s, Λ and $\bar{\Lambda}$ particles are not identified on a particle-by-particle basis. There is a large background from

- random combinations of unidentified daughter particles;
- uncorrelated identified daughter particles.

However, the yield can be estimated by counting the candidates within a mass window around the center of the signal peak above a fitted background line.

2.8.5.1 背景估计的旋转法

决定背景的一种可能方法是将所有的 positive 径迹绕着初级顶点旋转 180 度. 这种方法 destorys all the secondary vertices and only combinatorial background is reconstructed for the invariant mass distribution. We use a combination of a Gaussian function and a second order polynomial function to fit the invariant mass distributions.

2.9 Mass width and shift

We studied the mass width and shift from the invariant mass plots as a function of p_T. 主要研究动量分辨率的影响.

2.10 $\Xi^-\bar{\Xi}^+$ 的重构

Particles	Decay Channel	Branching ration
Ξ^-	$\Lambda\pi^-$	99.89%
$\bar{\Xi}^+$	$\bar{\Lambda}\pi^+$	99.89%

表 2.1: V0Xi

$\Xi^-(\Xi^+)$ 的衰变道如上表2.1所述. 其中 $\Lambda(\bar{\Lambda})$ 的重构要采取前面叙述的方法. 衰变的重构图如下:

图 2.6: VOXi

第3章　第三章

289

3.1　小节

290

第 4 章　第四章

4.1　小节

第 5 章　第五章

5.1　小节

第 6 章　关联之 HBT

6.1　干涉学介绍

HBT 首先利用两个光子之间的关联来确定实验源和天体源的角径。由于这种关联与同时存在两个时空点上测得的两粒子强度有关，故而称为强度干涉学，也称为 HBT 关联。人们发现在不同的能区中 HBT 半径随横动量增大而减小这一非常一致的趋势，这体现了发射原的横向和纵向的膨胀性。

人们认为在 RHIC 能区最高能量的碰撞下会发生从强子气体到部分子的转变。流体力学预言如果出现 QGP，粒子发射原的寿命会变长，空间尺度会变大，从而导致 HBT 半径增大，而 RHIC 的实验结果并没有看到这样的相变信号。S. Pratt 在流体力学模型框架下，通过综合的考虑初始条件、态方程、粘滞性对 HBT 半径的影响，发现 HBT 之谜也可以在流体力学模型的框架下得到解决。

强度干涉学的基本思想来源于使得波函数产生对称性的粒子全同原理。具体地说，就是要描述两个全同的玻色子的波函数要满足交换对称性，这就导致两粒子在小动量差附近被加强，而且这种加强于两粒子的空间分布直接相关。所以，可以利用两粒子动量空间的关联函数来得到坐标空间的信息。

6.2　关联函数

两个全同玻色子关联函数定义为：

$$C(p_1,p_2)=N\frac{P_2(\mathbf{p}_1,\mathbf{p}_2)}{P_1(\mathbf{p}_1)P_2(\mathbf{p}_2)} \tag{6.1}$$

其中，N 表示归一化系数，$P_x(\mathbf{p}_x)$ 和 $P_2(\mathbf{p}_1,\mathbf{p}_2)$ 分别为单粒子谱和两粒子谱。粒子谱的定义为：

$$P(\mathbf{p})=\int d^4xS(x,p) \tag{6.2}$$

$S(x,p)$ 为源函数。通过质壳关系和平滑近似我们可以得到：

$$C(\mathbf{q},\ \mathbf{K})-1=\frac{|\int d^4S(x,K)e^{iqx}|}{|\int d^4xS(x,K)|} \tag{6.3}$$

其中，$< ... >$ 表示对发射函数取平均，$q = p_1 - p_2$ 和 $K = (p_1 + p_2)/2$ 分别为两粒子的动量差和动量和。由于两粒子关联函数只有 3 个独立变量，而发射函数的时空分量包括四个变量 (x, t)。因此要从关联函数 C(q, K) 得到 S(x, K) 必须要包含一定的模型假设。利用所谓的“归一化相对距离分布]”:

$$d(x,K) = \int d^4X s(X + \frac{x}{2}, K)(X - \frac{x}{2}, K) \tag{6.4}$$

$$s(x,K) = \frac{S(x,K)}{\int d^4x S(x,K)} \tag{6.5}$$

其中 s(x, K) 为归一化发射函数。由于 d(x, K) 为偶函数，利用质壳关系，关联函数可以写成:

$$C(q,K) - 1 \int d^4 cos(q,x) \int dt d(x + \beta t, t; K) \tag{6.6}$$

由此，我们可以通过关联函数反推从而得到源函数。在实际过程中，人们并不是直接由关联函数出发重构反射源，而是先对反射函数时空结构进行一定的假设，找到其与 HBT 之间的关联关系，再反推回到发射源的时空信息。

高斯参数化是现阶段研究强度干涉学最主要的参数化公式。在高能重离子碰撞过程中产生的源具有膨胀性，在我们的认知中只有高斯形式能描述这种性质，因此就有必要来了解关联函数共和 HBT 半径的高斯参数化。选择合适的关联发射函数带入公式中，我们可以得到高斯形式的关联函数:

$$C(q,K) - 1 = exp[-q_u q_v \langle \widetilde{x}^u \widetilde{x}^v(K) \rangle] \tag{6.7}$$

其中 $\widetilde{x}$ 定义为时空点 x 相对于“有效发射中心”的距离。一般来说根据公式6.4得到的两粒子的平均动量 **K** 反应的半宽并不是真正源的大小。只有当反射源没有空间动量关联，即 $S(x,K) = f(x)g(x)$ 时得到的半宽才和源真正的半宽是一致的。受到质壳关系的限制，目前人们采用如下图的方式定义的高斯参数化得到“out-side-long(osl)”坐标系：long 方向与入射方向平行，out 方向与 K 的横向分量平行，side 方向垂直于 out,long，并且给出了相对动量差 q 的三个高斯分量 $q_{out}, q_{side}, q_{long}$。在“out-side-long(osl)”坐标系中，粒子对的时间分量通过质量约束可以忽略，从而得到关联函数的高斯参数化形式:

$$C(q,K) - 1 = exp[-\sum_{i,j=o,s,l} R^2_{ij}(K) q_i q_j] \tag{6.8}$$

其中 $R^2_{ij}(K)q_iq_j$ 的六个独立分量称为“HBT”半径，其形式可以写为:

$$R^2_{ij}(K)q_iq_j = \left\langle (\widetilde{x}_i - \beta_i \widetilde{t}_i)(\widetilde{x}_j - \beta_j \widetilde{t}_j) \right\rangle \qquad i,j = o,s,l \tag{6.9}$$

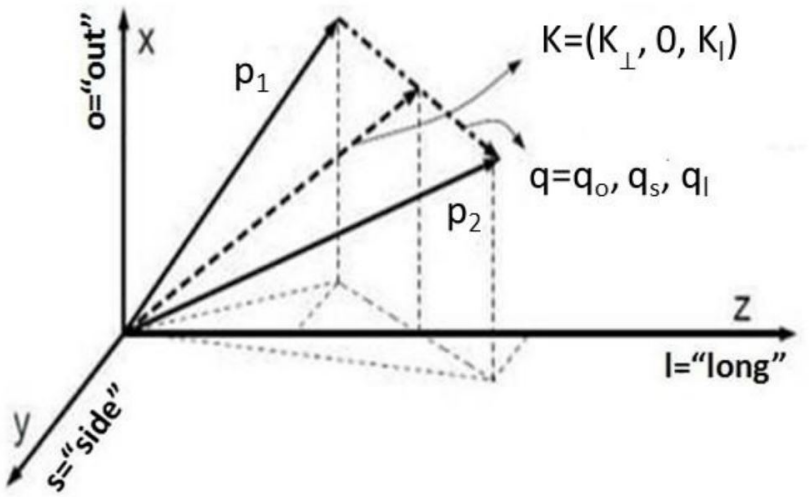

图 6.1: out-side-long 坐标系，其中纵向 (long) 沿着入射方向。

一般来说，C(q, K) 不仅依赖与粒子对平均动量 K 的横向分量 $K_\perp$ 和纵向分量 K_l 而且还依赖于横向动量 $K_\perp$ 与横向平面的夹角 Φ. 再对心碰撞中 (b˜0) 和 LCMS(longitudinally comoving system, $K_l = 0$) 坐标系中，会使交叉项消失，从而可以得到：

$$R_s^2(K) = \left\langle \widetilde{x_s}^2 \right\rangle (K) \tag{6.10}$$

$$R_o^2(K) = \left\langle (\widetilde{x_l} - \beta_o \widetilde{t})^2 \right\rangle (K) \tag{6.11}$$

$$R_l^2(K) = \left\langle \widetilde{x_l}^2 \right\rangle (K) \tag{6.12}$$

6.3 高斯热源模拟

由于高斯热源模型本身假定热源中粒子向外发射是各向同性的，而在火球产生之初粒子数在坐标空间沿各个方向分布应该是由中心向边缘递减，因此假定为高斯分布。在高斯热源模型中，粒子在坐标空间满足高斯分布：

$$f(r) = Ar^2 exp(-\frac{r^2}{2R^2}) \tag{6.13}$$

其中 A 为归一化常数，R、r 均为四维时空方差，表示高斯热源在时空上的大小。

通过分析静态高斯热源的时空分布和动量分布，我们对高斯热源的 HBT 关联进行分析。这里我们要用到分析 HBT 关联函数常用的三维拟合公式，这

个公式要用到前边所推导出的高斯参数化：

$$C(q,K) = 1 + \lambda exp(-R_{side}^2 q_{side}^2 - R_{out}^2 q_{out}^2 - R_{long}^2 q_{long}^2) \tag{6.14}$$

其中，q_{long} 是沿粒子入射方向的动量差。

6.4 原理

a schematic is shown of the HBT intensity interferometer.Here, waves emitted from sources **a** and **b** impinge on detectors **1** and **2**.The resulting amplitudes seen at each detector are given by:

$$A_1 = \frac{1}{L}(\alpha e^{i(pr_{1a}+\phi_a)} + \beta e^{i(pr_{1b}+\phi_b)}) \tag{6.15}$$

$$A_2 = \frac{1}{L}(\alpha e^{i(pr_{2a}+\phi_a)} + \beta e^{i(pr_{2b}+\phi_b)}) \tag{6.16}$$

其中 α 和 β represent the emission strengths at source points **a** and **b**,respectively, and ϕ_a and ϕ_b are the starting phases of the two waves as they are emitted from the two source points.In this example, both waves are assumed to have been emitted with the same momentum p.

The difference between Michelson and HBT interferometry comes about in how the intensities measured at detectors **1** and **2**:

$$I_1 = |A_1|^2 = \frac{1}{L^2}(|\alpha|^2 + |\beta|^2 + 2\Re[\alpha * \beta e^{i[p(r_{1b}-r_{1a})+(\phi_b-\phi_a)]}]) \tag{6.17}$$

$$I_2 = |A_2|^2 = \frac{1}{L^2}(|\alpha|^2 + |\beta|^2 + 2\Re[\alpha * \beta e^{i[p(r_{2b}-r_{2a})+(\phi_b-\phi_a)]}]) \tag{6.18}$$

$$\tag{6.19}$$

are used in the experiment.If the intensity is examined for a short time,the initial interference pattern will show itself due to the phase variation in the last term of equation.If the intensity is averaged over long times,these phases cancel due the randomness in ϕ_a and ϕ_b,and the interference fringes seen at the single detectors vanish:

$$\langle I_1 \rangle = \langle I_2 \rangle = \frac{1}{L^2}(|\alpha|^2 + |\beta|^2) \tag{6.20}$$

Examination of the coincidence rate, $\langle I_1 I_2 \rangle$, again averaged over long times,gives the product of the two single intensity measurements at the two detectors,plus

an extra term which depends on the physical extent of the source.Normalizing the coincidence rate by the product of the single intensities gives the correlation function,a direct link between the property of the source that is to be measured, namely its physical extent,and the observed data, or the measured intensities at two detectors:

$$C(\vec{R},\vec{d}) = \frac{\langle I_1 I_2\rangle}{\langle I_1\rangle \langle I_2\rangle} = 1 + \frac{2|\alpha|^2|\beta|^2}{(|\alpha|^2+|\beta|^2)^2} cos[p(r_{1a} - r_{2a} - r_{1b} + r_{2b})] \quad (6.21)$$

Equation 6.21 demonstates that correlations still exist even in time-averaged intensity measurements.Although this would prove useful in the astronomical measurements made by Hanbury Brown and Twiss,its most consequential impact would be in the realm of particle physics.Eventually, techniques were developed that allowed the amplitudes from widely spaced radio telescopes to be combined without loss of phase information,and Michelson interferometry soon emerged again as the primary method of determining angular diameters of stellar objects.

6.5 Theory of Identical Boson Interferometry

Pions emitted from a heavy-ion collision behave according to the QED equation of state for free-traveling particle, the Klein-Gordon equation:

$$\left(\frac{\partial^2}{\partial t^2} + \nabla^2 + m_\pi^2\right)\Phi(x) = J(x) \quad (6.22)$$

In this equation, J(x) represents the nuclear current operator acting as the source of pions,m_π is the mass of a pion and $\Phi(x)$ is the pion field.

6.6 Pion field Operators

The single and two-particle coincidence momentum probability distributions for pions are given below:

$$P_1(p) = E_p \frac{dN}{d^3p} = E_p \left\langle a_p^+ a_p \right\rangle \quad (6.23)$$

$$P_2(p_1,p_2) = E_{p_1}E_{p_2}\frac{dN}{d^3p_1 d^3p_2} = E_{p_1}E_{p_2}\left\langle a_{p_1}^+ a_{p_2}^+ a_{p_2} a_{p_1}\right\rangle \quad (6.24)$$

In the above equation, E_p is the energy of a pion with momentum p,and a_p^+, a_p represent the creation adn annihilation operators acting on a coherent state $|J>$,the solution to equation 6.22.One of the properties of $|J>$ is that it is an eigenstate of a_p,so that

$$a_p|J>= iJ(p)|J> \tag{6.25}$$

equation 6.25 allows an immediate computation of the probability distributions in equation 6.22. The two-pion correlation function $C(p_1, p_2)$ is the experimentally measured ratio of the two-pion coincidence momentum distribution to the single pion distribution,and for the above coherent state |j> it is found to be:

$$C(p_1, p_2) = \frac{P_2(p_1, p_2)}{P_1(p_1)P_2(p_2)} = \frac{\left\langle a_{p_1}^+ a_{p_2}^+ a_{p_2} a_{p_1} \right\rangle}{\left\langle a_{p_1}^+ a_{p_1} \right\rangle \left\langle a_{p_2}^+ a_{p_2} \right\rangle} = \frac{|J(p_1)|^2 |J(p_2)|^2}{|J(p_1)|^2 |J(p_2)|^2} = 1 \tag{6.26}$$

Thus, for pions behaving under the nuclear current operator in equation (6.22),there are no momentum correlations between pairs.In order to calculate the effect of pions emitted from a chaotic source,it is necessary to use superposition of classical sources distributed in phase space.By averaging over these sources, the two-particle momentum probability distribution (Equation 6.23) can be factorized as:

$$P_2(p_1, p_2) = E_{p_1} E_{p_2} \left\langle a_{p_1}^+ a_{p_2}^+ a_{p_2} a_{p_1} \right\rangle = E_{p_1} E_{p_2} \left[\left\langle a_{p_1}^+ a_{p_1} \right\rangle \left\langle a_{p_2}^+ a_{p_2} \right\rangle + \left\langle a_{p_1}^+ a_{p_2} \right\rangle \left\langle a_{p_2}^+ a_{p_1} \right\rangle \right] \tag{6.27}$$

This factorization assumes independent particle emission, or full sources chaoticity. It is one of the central assumptions of HBT.Another name for the factorization in equation (6.27) is the generalized Wick Theorem.Heuristically it can be seen as a description of the two possible paths two identical particles can take after being emitted from two source points and arriving at two detection points.

Using equation (6.27), the two-pion correlation function can be calculated for a chaotic source:

$$C_2(p_1, p_2) = \frac{P_2(p_1, p_2)}{P_1(p_1)P_1(p_2)} = 1 + \frac{|\left\langle a_{p_1}^+ a_{p_2} \right\rangle|^2}{\left\langle a_{p_1}^+ a_p \right\rangle \left\langle a_{p_2}^+ a_{p_2} \right\rangle} \tag{6.28}$$

The expectation values van be computed and related to the Wigner phase-space density,S(x, K),the quantum mechanical analogue of the classical phase-space density which is a function of both space x and total momentum K.The resulting expression is :

$$\sqrt{E_{p_i}E_{p_j}}\left\langle a^+_{p_i}a_{p_j}\right\rangle = \int S(x,K_{ij})e^{iq_{ij}x}d^4x \tag{6.29}$$

In this equation, $K_{ij} = \frac{p_i+p_j}{2}$ is the average momentum of a pair of pions i and j,and $q_{ij} = |p_i - p_j|$ is the invariant momentum difference of the pairs.Using equation (6.28) and (6.29) gives the expression for the two-pion correlation function in terms of the Wigner phase-space density:

$$C_2(p_1,p_2) = 1 + \frac{|\int d^4xS(x,K)e^{iq\cdot x}|^2}{\int d^4xS(x,p_1)\int d^4xS(x,p_2)} \tag{6.30}$$

In order to parameterize the two-pion correlation function in terms of the physical observable of pion momenta,the Wigner phase-space emission function $S(x,K)$ can be approximated by a Gaussian distribution.This results in a Gaussian correlation function in terms of the momentum difference $q = p_1 - p_2$:

$$C_2(\mathbf{q},\mathbf{K}) = 1 + e^{-q_uq_v\langle\widetilde{x}^u\widetilde{x}^v\rangle(\mathbf{K})} \tag{6.31}$$

其中, $\widetilde{x}^u$ describes the rms widths of effect sources of particles with total momentum $\mathbf{K}$. Different parameterizations can obtain these widths in a particular coordinate system to describe the size of the freeze-out region,however the widths obtained only describe the length of a "region of homogeneity"where particle pairs with momentum $\mathbf{K}$ are emitted.

6.7 Correlation function parameterizations Q_{inv}

The simplest Gaussian parameterization folds all length and time information into one length scale,extracted from a distribution of invariant four-momentum differences

$$Q_{inv} = \sqrt{|p_1 - p_2|^2 - (E_1 - E_2)^2}. \tag{6.32}$$

Once the correlation function has been computed,it is fit to the following equation:

$$C_2(q,K) = 1 + \lambda(K)e^{-Q^2_{inv}\cdot R^2_{inv}(K)} \tag{6.33}$$

The λ parameter in equation (6.33) represents the degree of contamination in the particle sample being studied,as well as a measure of the degree of chaoticity in the system.In a pure particle sample with ful chaoticity its value would be unity.Since the correlation function is one-dimensional, very few statistics are needed to obtain a high quality fit to the data,however since the fit parameter $R_{inv}(K)$ folds so much information into one variable,it is difficult draw a substantial conclusion about the properties of the source.

6.8 Pratt and Bertsch 参数化

A 3-dimensional cartesian parameterization, first used by S. Pratt and G. Bertsch,uses a coordinate system based on the pair momentum **k**. 看下图6.2, for every pair, The transverse momenta are further split into two components,one in the direction of pair and the other in the orthogonal direction.From these projections, the invariant momentum difference is calculated for each direction:k_T (out); $\perp$ to k_T (side); and parallel to the beam (long).These qualities are then used to produce a 3-dimension correlation function,which can be fit to:

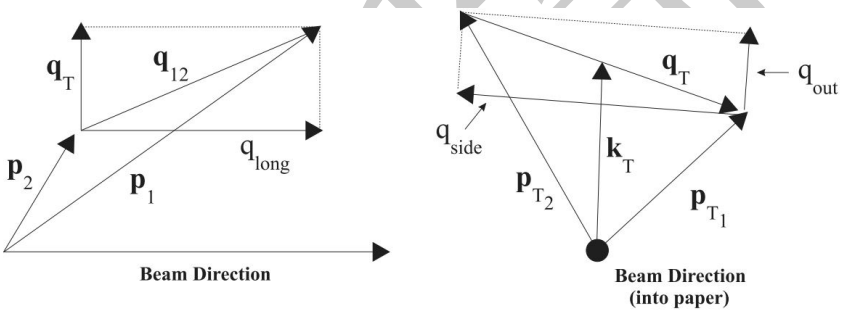

图 6.2: Bertsch-Pratt or cartesian parameterization of the two-pion correlation function.

$$C_2(q,K) = 1 + \lambda(K) e^{-q_{out}^2 \cdot R_{out}^2(K) - q_{side}^2 \cdot R_{side}^2(K) - q_{long}^2 \cdot R_{long}^2(K)} \tag{6.34}$$

Although all three radius parameters describe lengths of homogeneity along the three axes,$R_{out}(K)$ contains additional information about the lifetime of the source,due to the fact that this parameter is sensitive to pions which are created at a later time,traveling in the direction of **k** of the pion pair,where

$R_{side}(\mathbf{K})$ is sensitive only to those pions created at the periphery of the freeze-out region,at the onset of hadronization, and not to those created at later time.

The difference in sensitivity between $R_{out}(K)$ and $R_{side}(K)$ to the pions with delayed emission allows in a simplified picture for an estimate of the lifetime of the freeze-out source

$$R_{out}^2(K) - R_{side}^2(K) \approx \beta_\perp^2 \left\langle \tilde{t}^2 \right\rangle . \tag{6.35}$$

In this equation, $\beta_\perp^2$ is the transverse velocity of pair,and $\left\langle \tilde{t}^2 \right\rangle$ is the average emission duration of the source.Estimating the lifetime with equation (6.35) assumes that $R_{out}(K)$ and $R_{side}(K)$ measure approximately the same physical homogeneity length of the source.This can be a faulty assumption if the source is opaque, 见下图6.3 in which case $R_{side}(\mathbf{K})$ would measure a much larger homogeneity length than $R_{out}(K)$,resulting in an imaginary emission lifetime.

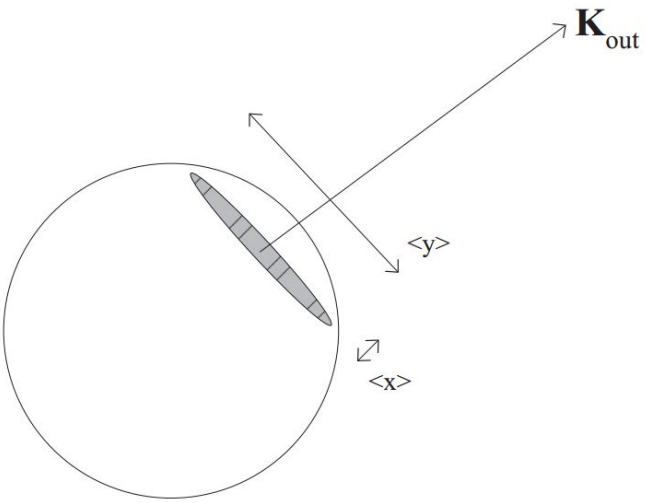

图 6.3: Opaque source, in which R_{side} measures the homogeneity length of the source, but R_{out} is sensitive only to the surface thickness, denoted by $\langle x \rangle$.

第7章　集体流

7.1　cumulant method

在重离子碰撞中观测粒子的集体运动是研究碰撞中产生的高温高密物质的有效方法。集体运动的各向异性是非对心碰撞初期产生的物质在坐标空间的各向异性的结果，动量空间的各向异性已经在 RHIC，LHC 实验中观测到。

实验上产生的粒子可以用表示为:

$$E\frac{d^3N}{d^3p} = \frac{1}{2\pi}\frac{d^2N}{p_t dp_t dy}\left(1+\sum_{n=1}^{\infty}2v_n cos(n(\phi-\Psi_R))\right) \tag{7.1}$$

其中 E 是粒子的能量，$\vec{p}$ 为粒子的三动量，p_t 是粒子的横动量，ϕ 是粒子的方位角，y 是粒子的快度，Ψ_R 事件的反应平面。公式中傅里叶系数 v_n 表示各向异性流。一阶系数 v_1 称为直接流。二阶系数 v_2 称为椭圆流。另一方面如果我们只对平均值感兴趣的化，我们可以将它们称为 reference 流。单个事件平均的傅里叶系数为: $< v_n >$

第 8 章　RHIC 实验设备

8.1　加速器设备

Colliding ions in RHIC is a multi-step process. Negatively charged ions (A^{-1} or d^{-1} for example) from a pulsed sputter ion source are partially stripped of their eletrons and then accelerated in the Tandem van de Graaff. After further stripping (for gold ions this corresponds to a charge state of +32) at the exit of the Tandem, the ions are delivered to the Booster Synchrotron where they are accelerated more. The ions are stripped again at the exit of the Booster (eg. gold ions reach a +77 charge state at this stage) and injected to the AGS for acceleration to the RHIC injection energy. Fully stripped state (+79 for gold ions) is reached at the exit of the AGS. In p+p collisions, the protons are injected into the Booster Synchrotron directly from the LINAC (LINear ACcelerator), accelerated in the AGS and finally injected in the RHIC. The Collider itself consists of two concentric accelerator/storage rings on a horizontal plane, one for clockwise and the other for counter-clockwise beams. The rings are oriented so that they intersect with one another at six locations along their 3.8 km circumference. 1740 superconducting magnets are required in order to bend, focus and steer the beams to a co-linear path for head-on collisions.

8.2　STAR Detector

The Solenoidal Tracker at RHIC (STAR) was designed primarily for measurements of hadron production over a large solid angle, featuring detector systems for high precision tracking, momentum analysis, and particle identification in a region surrounding the center-of-mass rapidity. The large acceptance of STAR (complete azimuthal symmetry $\Delta\Phi = 2\pi$ and a pseudo-rapidity range $|\eta| < 4.$) makes it particularly well suited for single event characterization of

heavy ion collisions and for the detection of hadron jets. Its main components are a large Time Projection Chamber(TPC), a Silicon Vertex Tracker (SVT), two smaller radial Forward and Backward TPCs(FTPCs), a Time of Flight patch (TOF) and an Electromagnetic Calorimeter (EMC) inside a 0.5T magnetic field.

第 9 章　零碎知识

9.1　碰撞的非弹种类

According to hadronic cross section, elastic and in-elastic collisions are sorted. For in-elastic collisions, there are singly-diffractive, double-diffractive and non-diffractive processes. Diffractive processes are difined as processes where one nucleon acts as a region of absorption and the interference of scattering amplitudes gives rise to diffraction pattern in the forward and backward regions. A nucleon suffering a diffractive scattering becomes excited and then loses a small amount of energy when breaking up into a few particles at a small emission angle. This can occur in one of the nucleons (singly) or in high both (doubly). In non-diffractive processes the nucleons hit "head-on" and both disintegrate creating large particle multiplicities at mid-rapidity. The STAR p+p trigger is only sensitive to the *non-singly diffractive (NSD)* cross-section (σ_{NSD}), since it requires charged tracks to be detected in coincidence on both sides of the interaction point, so about 70% of the inelastic cross-section (σ_{inel}) are measured at STAR.

9.2　V0 decays

The appearance of the decay of an unobserved neutral strange particle into two observed charged daughter particles gives rise to the terminology "V0" to describe the decay topology. The following neutral strange species have been analysed:

不可观测的中性奇异粒子衰变为两个带电荷的可观测的 daughter particles, 我们用术语'V0' 来描述这种衰变形式: Candidate V0s are formed by combining together all possible pairs of opposite chapter-sign tracks in an event. The invariant mass of the V0 candidate under different decay hypotheses can then be determined from the track momentum and the daughter masses(e.g. for Λ

Species	Decay channel	Branching ratio
K^0_S	$\pi^+ + \pi^-$	0.692
Λ	$p + \pi^-$	0.639
$\bar{\Lambda}$	$\bar{p} + \pi^+$	0.639

表 9.1: V0 decay

the positive daughter is assumed to be a proton, the negative daughter a π^-). The spectra contain three contributions:

- real particles of the species of interest;
- neutral strange particles of a different species;
- conbinatorial background from chance positive/negative track crossings.

Selection cuts are the applied to the candidates to suppress the background whilst maintaining as much signal as possible. There are two methods for reducing background.

- energy-loss particle identification.
- geometrical cuts on the V0 candidates.

9.3 衰变特性

重子	主要衰变方式	分值比 (%)
n	$pe^-\bar{\upsilon}_e$	100
Λ	$p\pi^-$	63.9
	$n\pi^0$	35.8
Σ^+	$p\pi^0$	51.57
	$n\pi^+$	48.31
Σ^0	$\Lambda\gamma$	100
Σ^-	$n\pi^-$	99.848
Ξ^-	$\Lambda\pi^-$	99.887
Ξ^0	$\Lambda\pi^0$	99.54
Ω	ΛK^-	67.8
	$\Xi\pi^-$	23.6

表 9.2: baryon

表 9.3: meson

第 10 章　附录

10.1　附录 A:

参考文献

[1] C. Adler, Z. Ahammed, C. Allgower, et al. Azimuthal anisotropy of K^0_S and $\Lambda + \overline{\Lambda}$ production at midrapidity from Au + Au collisions at $\sqrt{s_{NN}} =$ 130GeV. *Phys. Rev. Lett.*, 89:132301, Sep 2002. 14